

Reproduced by



CENTRAL AIR DOCUMENTS OFFICE

WRIGHT-PATTERSON AIR FORCE BASE - DAYTON, OHIO

REEL-8

2729 B

A.T.I

58417

The
U.S. GOVERNMENT

IS ABSOLVED

FROM ANY LITIGATION WHICH MAY ENSUE FROM ANY
INFRINGEMENT ON DOMESTIC OR FOREIGN PATENT RIGHTS
WHICH MAY BE INVOLVED.

UNCLASSIFIED

Measurement of Bubble Pulse Phenomena IV: Pressure-Time Measurements in Free Water

58417

Arons, A. B.; Slifko, J. P.; Carter, A. H.; and others

(None)

Woods Hole Oceanographic Inst., Underwater Explosives Research *

(None)

Bureau of Ordnance, Washington, D. C.

NAVORD-408

Nov '47 Unclass. U.S. English 42 tables, diagrs, graphs

Bubble pulse pressure-time measurements have been made with 0.5, 2.5 and 12.0 lb TNT charges at depths of 250 and 500 ft. It was found that even at 500 ft, there is sufficient migration to prevent accurate scaling of the peak pressure of the bubble pulses. The migration does not appreciably affect either the impulse or the energy flux, and the latter quantities follow the ideal scaling law within the available precision of measurement. Experimental results tabulated include peak pressure, migration, impulse, energy flux, and composite pressure-time curves for the first two bubble pulses.

* Laboratory, Mass.

LIMITED. Requests for copies must be routed through Chief, BuAer for approval.

Navy Materiel (28)
Naval Ordnance (1)

Explosives, Underwater - Gas pressure effect (34470); Explosions - Shock and pressure measurement (34458); Pressure waves (74320)

Air Division
RECEIVED

13279

ATI No. 58417

NAVORD REPORT 408

MEASUREMENT OF BUBBLE PULSE

PHENOMENA IV: PRESSURE-TIME

MEASUREMENTS IN FREE WATER



BUREAU OF ORDNANCE PUBLICATION

6 NOVEMBER 1947

FOREWORD

1. NavOrd 408 is Part IV of a series of reports on the measurement of bubble-pulse phenomena of an underwater explosion. Experimental results tabulated in this report include peak pressure, impulse, energy flux, migration, and composite pressure-time curves for the first two bubble pulses.
2. The findings herein represent the interpretations and conclusions of the authors and are not necessarily those of the Bureau of Ordnance.
3. This report does not represent a final and comprehensive study. Comment from other agencies is invited.


S. H. Crittenden, Jr.
Captain, U. S. Navy
Chief, Ammunition
and Explosives Section

6 November 1947

13279

NAVY DEPARTMENT
BUREAU OF ORDNANCE
WASHINGTON, D.C.

Rear Admiral A.G. Noble, USN
Chief of the Bureau of Ordnance

Captain K. H. Noble, USN
Assistant Chief of Bureau for Research

Captain S. H. Crittenden, Jr., USN
Ammunition and Explosives

Dr. Stephen Brunauer
High Explosives and Amphibious Munitions

NAVORD REPORT 408

MEASUREMENT OF BUBBLE PULSE PHENOMENA IV:
PRESSURE-TIME MEASUREMENTS IN FREE WATER

by

A. B. Arons, J. P. Slifko, A. H. Carter, D. R. Yennie, and C. L. Wingate

Underwater Explosives Research Laboratory
Woods Hole Oceanographic Institution
Woods Hole, Massachusetts

Paul M. Fye
Director of Research

6 November 1947

TABLE OF CONTENTS

	<u>Page</u>
Abstract	
I. INTRODUCTION	1
II. PERIODS OF OSCILLATION	2
III. PEAK PRESSURES: FIRST AND SECOND BUBBLE PULSES	10
IV. POSITIVE IMPULSE AND ENERGY FLUX	12
V. MEASUREMENT TECHNIQUES	16
VI. SUMMARY AND CONCLUSIONS	19
APPENDIX I THE PULSATING STATIONARY GAS GLOBE	21
APPENDIX II TABULATION OF ORIGINAL DATA	27
APPENDIX III COMPOSITE CURVES	32
LIST OF REFERENCES	41

LIST OF TABLES

Table	Page
I SUCCESSIVE BUBBLE PERIODS (0.505 lbs. TNT at 250 ft.)	2
II SUCCESSIVE BUBBLE PERIODS (2.507 lbs. TNT at 250 ft.)	4
III SUCCESSIVE BUBBLE PERIODS (0.505 lbs. TNT at 500 ft.)	4
IV SUCCESSIVE BUBBLE PERIODS (2.507 lbs. TNT at 500 ft.)	5
V SUCCESSIVE BUBBLE PERIODS (12.01 lbs. TNT at 500 ft.)	6
VI SUMMARY OF PERIOD CONSTANTS	7
VII RATIOS OF SUCCESSIVE BUBBLE PERIODS	7
VIII SUCCESSIVE BUBBLE PERIODS (0.505 lbs. TNT at 400 ft.)	8
IX APPARENT BUBBLE MIGRATION AND CORRECTED PEAK PRESSURES	10
X BUBBLE PULSE PEAK PRESSURES FOR VARIOUS CHARGE ORIENTATION	12
XI REDUCED POSITIVE IMPULSE: FIRST AND SECOND BUBBLE PULSES	13
XII VARIATION OF POSITIVE IMPULSE WITH DEPTH OF DETONATION: FIRST BUBBLE PULSE	14
XIII REDUCED ENERGY FLUX: FIRST AND SECOND BUBBLE PULSES	15
A-I NEGATIVE PRESSURE AT BUBBLE MAXIMUM FOR VARIOUS CHARGE DEPTHS	26
A-II FIRST AND SECOND BUBBLE PULSE PEAK PRESSURES: 0.505 lbs. TNT at 250 ft.	28
A-III FIRST AND SECOND BUBBLE PULSE PEAK PRESSURES: 2.507 lbs. TNT at 250 ft.	28
A-IV FIRST AND SECOND BUBBLE PULSE PEAK PRESSURES: 0.505 lbs. TNT at 500 ft.	29
A-V FIRST AND SECOND BUBBLE PULSE PEAK PRESSURES: 2.507 lbs. TNT at 500 ft.	30
A-VI FIRST AND SECOND BUBBLE PULSE PEAK PRESSURES: 12.01 lbs. TNT at 500 ft.	31
A-VII FIRST AND SECOND BUBBLE PULSE PEAK PRESSURES: 0.505 lbs. TNT at 400 ft.	31

LIST OF FIGURES

Figure		Page
1	PRESSURE-TIME RECORD SHOWING SHOCK WAVE AND BUBBLE PULSES	3
2	PERIOD CONSTANTS AND SUCCESSIVE PERIOD RATIOS VS. PULSE NUMBER	9
3	RIG FOR FREE WATER BUBBLE SERIES	17
A-1	COMPOSITE BUBBLE PULSE CURVES: PRESSURE VS TIME CHARGE DEPTH 250 ft., GAUGE POSITION G-1	33
A-2	COMPOSITE BUBBLE PULSE CURVES: PRESSURE VS TIME CHARGE DEPTH 250 ft., GAUGE POSITION G-2,3	34
A-3	COMPOSITE BUBBLE PULSE CURVES: PRESSURE VS TIME CHARGE DEPTH 250 ft., GAUGE POSITION G-4	35
A-4	COMPOSITE BUBBLE PULSE CURVES: PRESSURE VS TIME CHARGE DEPTH 500 ft., GAUGE POSITION G-1	36
A-5	COMPOSITE BUBBLE PULSE CURVES: PRESSURE VS TIME CHARGE DEPTH 500 ft., GAUGE POSITION G-2	37
A-6	COMPOSITE BUBBLE PULSE CURVES: PRESSURE VS TIME CHARGE DEPTH 500 ft., GAUGE POSITION G-2,3	38
A-7	COMPOSITE BUBBLE PULSE CURVES: PRESSURE VS TIME CHARGE DEPTH 500 ft., GAUGE POSITION G-3	39
A-8	COMPOSITE BUBBLE PULSE CURVES: PRESSURE VS TIME CHARGE DEPTH 500 ft., GAUGE POSITION G-4	40

Abstract

Bubble pulse pressure-time measurements have been made with 0.5, 2.5, and 12.0 lb. TNT charges at depths of 250 and 500 ft. It is found that even at 500 ft., there is sufficient migration to prevent accurate scaling of the peak pressure of the bubble pulses. The migration, however, does not appreciably affect either the impulse or the energy flux, and the latter quantities follow the ideal scaling law within the available precision of measurement.

Experimental results tabulated in this report include peak pressure, migration, impulse, energy flux, and composite pressure-time curves for the first two bubble pulses.

BUBBLE PULSE PHENOMENA IV:

PRESSURE-TIME MEASUREMENTS IN FREE WATER

I. INTRODUCTION

1.

The gas globe produced in an underwater explosion tends to migrate vertically upwards under the influence of gravity. In the process of migration, some of the potential energy stored in the water by the initial radial expansion of the bubble is converted into kinetic energy of the vertically moving water. This energy is not restored to the bubble as it collapses, and hence the amplitude of the first bubble pulse is less than it would have been had no migration occurred.

From the foregoing, it is evident that the pressure pulse will be at its maximum under conditions which make the bubble migration negligible or cause it to be in a "rest position". It is known that for relatively small charges a rest position occurs at a certain critical depth below the water surface due to the balancing of gravitational effects by the repulsion from the free surface¹⁾*. However, accurate pressure-time measurements under these circumstances are not possible because proximity to the free surface causes serious interference from the surface reflection of the pressure wave.**

Since the migration decreases with increasing depth of detonation, it should be possible to perform experiments at depths sufficiently great to make the migration effects negligible, or at least low enough so that only a small theoretical correction is needed to obtain the stationary bubble results.

2.

It was the object of the present investigation to obtain measurements at conditions of low migration in order to test the scaling of the bubble pulse parameters with charge size and to obtain better impulse and energy flux data than have heretofore been available for the stationary bubble. Such tests cannot be made directly on the migrating bubble, because the gravitational effect does not scale with charge size.

Three charge sizes were used: 0.505 lb, 2.507 lb, and 12.01 lb of cast TNT, and measurements were made at a depth of 500 ft in water having an overall depth in excess of 700 ft. (Surface and bottom effects were consequently negligible.) The half-pound charge is deemed to be the

* All such numbers refer to List of References at the end of this report.

** It should be noted that we are here concerned only with the normal bubble pulse and not with the so-called "anomalous pulse" occurring in proximity to free surfaces^{1,2,3}).

smallest which can be reliably detonated under these circumstances. The 12 lb charge is the largest that could be tolerated at a distance of 500 ft below the vessel performing the experiments; thus the range of charge size was the widest attainable with the available experimental equipment. The $\frac{1}{2}$ lb and $2\frac{1}{2}$ lb charge sizes were also studied at a depth of 250 ft. All pressure-time measurements were made at a distance from the charge such that the value of $W^{1/3}/R$ was kept constant at 0.352, W being the charge weight in pounds and R the distance from the center of the charge to the gauge in feet.

A typical pressure-time record is shown in Fig. 1. Periods of pulsation have been measured to the seventh, and in some cases to the eighth, bubble pulse. Peak pressures, impulse, and energy flux have been obtained for the first and second pulses.

II. PERIODS OF OSCILLATION

3.

The results of bubble period measurements are given in Table I through VII. The following notation applies to these tables:

T_n = period of n-th oscillation (msec)

σ_m = standard deviation of the mean

$T_n = (10^3) K_n W^{1/3}/D_o^{5/6}$

W = charge weight (lb)

D_o = absolute hydrostatic depth in ft (depth below the surface + 33)

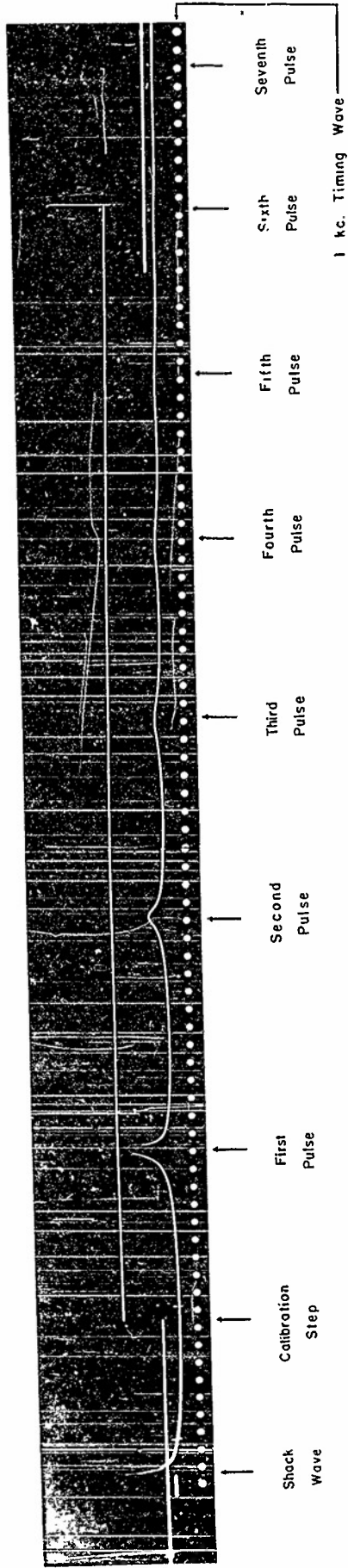
K_n = period constant of n-th oscillation

Table I

SUCCESSIVE BUBBLE PERIODS

0.505 lb TNT at 250 ft
($D_o = 283$ ft)

Shot No.	PERIODS (msec)						
	T_1	T_2	T_3	T_4	T_5	T_6	T_7
734	31.9	23.1	18.8	17.7	16.4	15.7	--
735	31.3	22.4	18.2	16.7	15.5	--	--
736	31.6	22.8	18.5	17.1	15.4	14.8	14.5
737	31.4	22.6	18.4	17.1	15.2	14.8	13
Avg.	31.6	22.7	18.5	17.2	15.6	15.1	13.8
σ_m	0.1	0.2	0.1	0.2	0.3	0.3	0.8
K_n	4.36	3.14	2.56	2.38	2.16	2.08	1.91



Charge: 0.505 lb TNT

Gauge dist: 2.25 ft

Depth: 500 ft

Fig. 1 Pressure-Time Record Showing Shock Wave and Bubble Pulses

Table II
 SUCCESSIVE BUBBLE PERIODS

2.507 lb TNT at 250 ft

($D_0 = 283$ ft)

Shot No.	PERIODS (msec)						
	T ₁	T ₂	T ₃	T ₄	T ₅	T ₆	T ₇
738	52.7	38.2	31.3	28.8	27.4	24.6	22.8
739	52.8	38.6	31.3	29.3	28.5	25.2	25
Avg	52.75	38.4	31.3	29.0	28.0	24.9	24
K _n	4.27	3.11	2.53	2.35	2.25	2.02	1.94

Table III
 SUCCESSIVE BUBBLE PERIODS

0.505 lb TNT at 500 ft

($D_0 = 533$ ft)

Shot No.	PERIODS (msec)							
	T ₁	T ₂	T ₃	T ₄	T ₅	T ₆	T ₇	T ₈
713	18.6	13.2	10.8	9.8	9.0	8.0	---	---
714	18.4	13.0	10.6	9.8	9.0	8.4	7.7	---
716	18.5	13.0	10.6	9.8	9.0	8.2	---	---
717	18.8	13.2	10.8	10.0	9.2	8.7	---	---
729	18.6	13.0	10.6	10.2	9.6	8.5	8.2	7.7
730	18.7	13.0	10.7	10.0	9.2	8.6	8.0	---
731	18.8	13.2	10.8	9.9	9.2	8.5	8.5	8.5
732	18.8	13.1	10.9	9.9	9.4	8.4	8.0	---
Avg	18.65	13.09	10.72	9.92	9.20	8.41	8.1	8.1
σ_m	0.05	0.04	0.04	0.05	0.07	0.08	0.1	---
K _n	4.36	3.06	2.51	2.32	2.15	1.97	1.90	1.9

Table IV
 SUCCESSIVE BUBBLE PERIODS

2.507 lb TNT at 500 ft

($D_0 = 533$ ft)

Shot No.	PERIODS (msec)						
	T_1	T_2	T_3	T_4	T_5	T_6	T_7
701	31.1	22.4	18.1	16.8	16.0	14.1	-----
702	31.2	22.6	18.1	17.1	16.2	14.8	-----
709	30.8	22.0	17.9	16.6	15.4	15.5	-----
710	31.2	22.7	18.2	16.6	15.2	14.2	-----
711	31.2	22.6	18.3	16.9	16.0	15.6	-----
712	31.0	22.2	18.2	16.8	15.8	14.8	-----
725	31.0	22.0	17.8	16.6	15.8	14.0	-----
726	30.9	22.2	18.0	16.6	15.8	14.2	-----
727	31.2	22.0	18.0	16.7	16.0	14.9	-----
728	31.3	22.6	18.3	17.4	16.4	14.6	15
740	31.2	22.2	18.0	16.8	15.6	14.2	14.5
741	31.1	22.4	18.4	16.9	15.2	15.0	-----
Avg	31.10	22.32	18.11	16.82	15.8	14.7	15
σ_m	0.05	0.08	0.05	0.07	0.1	0.1	-----
K_n	4.26	3.06	2.48	2.31	2.17	2.02	-----

Table V

SUCCESSIVE BUBBLE PERIODS

12.01 lb TNT at 500 ft

 $(D_0 = 533 \text{ ft})$

Shot No.	PERIODS (msec)							
	T ₁	T ₂	T ₃	T ₄	T ₅	T ₆	T ₇	T ₈
703	52.8	39.5	31.3	29.0	27.8	-----	-----	-----
706	52.7	39.3	31.3	29.2	27.7	26	24.5	20
707	52.4	39.4	31.6	28.2	26.0	24.5	-----	-----
708	52.6	39.4	31.6	28.5	26.0	-----	-----	-----
718	52.7	39.0	31.4	29.1	26.6	25.0	24.4	22
720	52.5	39.2	31.7	29.6	26.5	24.8	23	-----
721	52.8	39.0	31.5	29.4	26.4	24.8	24	-----
722	53.0	39.2	31.4	29.9	27.5	25.5	23	21.5
723	53.0	39.0	31.6	30.3	25.7	25.5	23	23
724	52.6	38.6	31.5	29.5	25.5	25.2	24	20
742	52.5	39.2	31.4	29.8	26.4	25.2	23.8	-----
743	52.8	39.2	31.5	30.1	26.7	24.7	24.5	-----
Avg	52.70	39.17	31.48	29.4	26.6	25.1	23.8	21.3
σ_m	0.06	0.06	0.04	0.2	0.2	0.1	0.2	0.6
K_n	4.29	3.19	2.56	2.39	2.16	2.04	1.94	1.73

Table VI
SUMMARY OF PERIOD CONSTANTS

Charge Weight (lb)	Depth (ft)	PERIOD CONSTANT							
		K ₁	K ₂	K ₃	K ₄	K ₅	K ₆	K ₇	K ₈
0.505	250	4.36	3.14	2.56	2.38	2.16	2.08	1.91	---
	500	4.36	3.06	2.51	2.32	2.15	1.97	1.90	1.9
2.507	250	4.27	3.11	2.53	2.35	2.25	2.02	1.94	---
	500	4.26	3.06	2.48	2.31	2.17	2.02	---	---
12.01	500	4.29	3.19	2.56	2.39	2.16	2.04	1.94	1.73
Avg	---	4.31	3.11	2.53	2.35	2.18	2.03	1.92	1.8

Table VII
RATIOS OF SUCCESSIVE BUBBLE PERIODS

Charge Weight (lb)	Depth (ft)	PERIOD RATIOS						
		K ₂ /K ₁	K ₃ /K ₂	K ₄ /K ₃	K ₅ /K ₄	K ₆ /K ₅	K ₇ /K ₆	K ₈ /K ₇
0.505	250	0.720	0.815	0.930	0.908	0.963	0.918	---
	500	0.702	0.820	0.924	0.927	0.916	0.964	1.0
2.507	250	0.728	0.814	0.929	0.957	0.898	0.960	---
	500	0.718	0.810	0.931	0.939	0.931	---	---
12.01	500	0.744	0.802	0.934	0.904	0.944	0.951	0.89
Avg	---	0.722	0.812	0.930	0.927	0.930	0.948	0.94

The value $K_1 = 4.36$ for half-pound charges agrees exactly with previous results (4). It will be noted in Table VI that the values of K_1 for the 2.5 and 12 lb charges are significantly lower than the 0.5 lb result. The reproducibility of the period measurements and the fact that the charge sizes were alternated in a definite sequence during the shooting program indicate that the difference cannot be due to systematic error in the determination of the depth of the charge. The discrepancy can only be interpreted as a slight but significant departure from the cube root law of variation of period with charge weight.

4.

Figure 2 shows a plot of average K_n vs pulse number and successive period ratio vs pulse number. The ratio rises rapidly for the first three pulses and then proceeds to rise very slowly, being significantly below unity even at the seventh pulse. The same effect is evident in the plot of K_n ; the value of the period constant continues to decrease in such a way that these results cannot be used to obtain a limiting value of K corresponding to the period of the ultimate small amplitude oscillations.

5.

Table VIII shows results obtained with two 0.505 lb TNT charges which were improperly boosted in that the 44 gm pressed tetryl pellet was positioned near the center of the cast TNT charge rather than near the top. (Previous experience at this laboratory has indicated that the latter type of boosting is more effective.)

Table VIII

SUCCESSIVE BUBBLE PERIODS

0.505 lb TNT at 400 ft

(Booster pellet improperly positioned)

Shot No.	PERIODS (msec)						
	T_1	T_2	T_3	T_4	T_5	T_6	T_7
698	20.74	14.86	11.70	11.15	10.65	10.0	9.2
699	20.69	14.80	11.80	11.0	10.1	9.9	9.6
Avg	20.71	14.83	11.75	11.08	10.4	10.0	9.4
K_n	4.00	2.74	2.17	2.06	1.92	1.84	1.74

Comparison of Tables VI and VIII shows that the values of K_n in Table VIII are systematically lower in all cases. This tends to confirm previous boosting experience since the low period constant is evidence of low energy release.

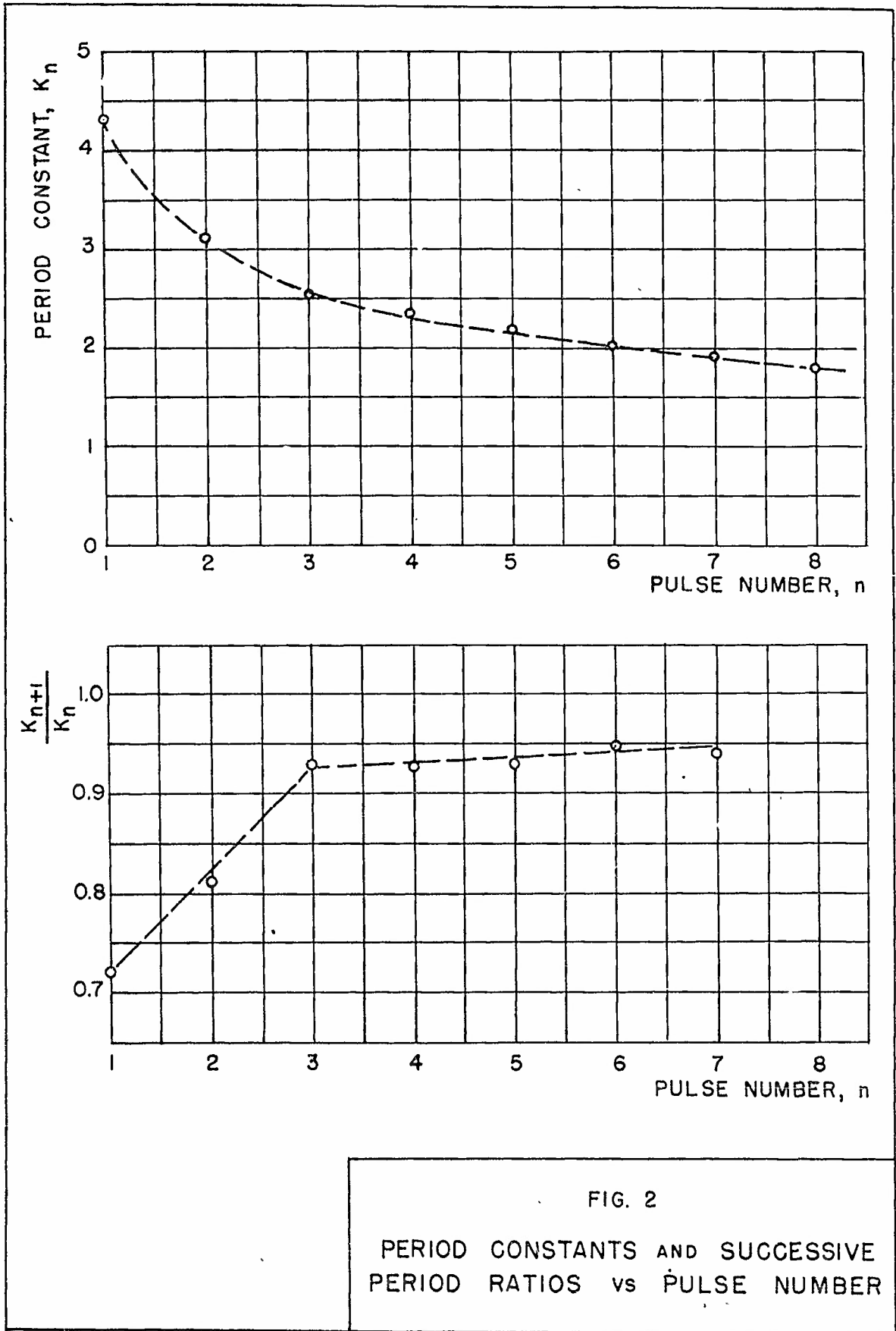


FIG. 2
 PERIOD CONSTANTS AND SUCCESSIVE
 PERIOD RATIOS vs PULSE NUMBER

III. PEAK PRESSURES: FIRST AND SECOND BUBBLE PULSES

6.

The original, uncorrected peak pressure data are tabulated in Appendix II. A summary of final, corrected peak pressure values appears in Table IX.

Table IX

APPARENT BUBBLE MIGRATION AND CORRECTED PEAK PRESSURES

h = vertical displacement of bubble from initial charge position at time of bubble minimum (ft)
 ΔP = excess peak pressure (lb/in.²) at $R = W^{1/3}/0.352$
 R = distance from center of bubble, (ft)
 σ_m = standard deviation of the mean

Charge Weight (lb)	Depth (ft)	First Pulse			Second Pulse		
		h (ft)	ΔP (lb/in. ²)	σ_m (%)	h (ft)	ΔP (lb/in. ²)	σ_m (%)
0.505	250	0.32	1120	1.4	0.51	225	2.2
2.507	250	0.80	1020	0.6	1.12	215	2.3
0.505*	400	0.15	1035	—	0.40	215	—
0.505	500	0.11	1210	0.5	0.16	250	2.0
2.507	500	0.32	1160	0.9	0.47	245	2.4
12.01	500	0.86	1140	0.9	0.79	260	2.3

*Charges improperly boosted.

The arrangement of charge and gauges is described in Sec. 16. Vertical migration of the bubble was calculated from the peak pressure values obtained on pairs of gauges vertically above and below the charge (Positions G1 and G4). It was assumed that the difference between average pressures at these two positions was due only to displacement of the bubble, and the pressure was assumed to vary inversely as the distance. This treatment neglects any effects due to asymmetry of the pressure field, but it appears to be justified by the fact that when pressures at G1 and G4 are corrected to the same distance as pressures measured off the cylindrical sides of the charge, all the values agree within the experimental scatter.

All the pressure values cited in Table IX correspond to the average of measurements made off the cylindrical sides of the charge and are corrected (by means of the migration values) to a distance from the bubble given by $R=W^{1/3}/0.352$.

Due to uncertainty in the exact location of the true baseline on the individual photographic records, the records were read with respect to an arbitrary baseline and were then adjusted to the theoretical base line values calculated in Appendix I.

7.

Perfect scaling would require that all the peak pressure values at a given $w^{1/3}/R$ be equal regardless of charge size. Examination of Table IX shows that this is not the case, and the principal cause of the observed variation is undoubtedly the migration of the bubble. In Chapter II it was shown that the period constants for the 2.5 and 12 lb charges were about 2% lower than that for the 0.5 lb charges. From this result one might expect the peak pressures of the larger charges to be lower by about the same percentage, but the observed effect is much too large to be accounted for by this mechanism alone.

Theoretical calculation of the influence of migration on the peak pressure^{5,6)} predicts effects very much less than those indicated in Table IX, the expected decrease in peak pressure for the worst case (2.5 lb at 250 ft) being less than 1%. The observed effect in this case seems to be at least 15%, if ΔP for the 0.5 lb charge at 500 ft is used as a basis of comparison.

The interpretation which must be placed on the results of Table IX is that the peak pressure does not scale well, even at conditions of relatively low migration. The effect can be minimized by going to still greater depth, although the gross variation of 6% between the 0.5 and 12 lb charges at 500 ft is not serious for most practical model work.

8.

The migration and pressure for the second pulse of the 12 lb charge are inconsistent with the other data. The discrepancy is probably due to a systematic error introduced in adopting a baseline in reading the original records.

It will be noted that the pressures for the improperly boosted 0.5 lb charges are significantly lower than the migration would indicate (by direct comparison with other observed migrations), thus confirming the results discussed in Sec. 5.

9.

As indicated in Sec. 16, the spherical symmetry of the pressure field was investigated by means of measurements off the cap and butt ends of the charge as well as off the cylindrical sides.

A comparison of pressures obtained in the various orientations is given in Table X.

Table X

BUBBLE PULSE PEAK PRESSURES FOR VARIOUS CHARGE ORIENTATION

Position of measurement defined by:

G2,3: Off cylindrical sides of charge

G2: Off cap end of charge

G3: Off butt end of charge

All values corrected to distance from bubble given by $R = W^{1/3}/0.352$ (ft)

Charge Weight (lb)	Depth (ft)	Peak Pressures (lb/in. ²)					
		First Pulse			Second Pulse		
		G2	G2,3	G3	G2	G2,3	G3
0.505	500	1365	1210	1095	285	250	230
2.507	500	1200	1160	1150	280	245	240
12.01	500	1200	1140	1120	295	260	250

Examination of Table X shows that the pressure off the cap end is systematically higher, and that off the butt end systematically lower, than the pressure off the cylindrical sides. The effect is most pronounced with the 0.5 lb charges and is relatively small for the 2.5 and 12 lb charges.

IV. POSITIVE IMPULSE AND ENERGY FLUX

10.

An enlarger was used to project the individual photographic records on graph paper, and pressure-time values were tabulated at intervals along the trace. Time was always measured with respect to the peak of the pulse, since this was the sharpest reference point available. Tabulations of individual records were then combined by averaging all ordinates at corresponding times for the various gauge positions and charge sizes. Thus a group of composite pressure-time curves was obtained, each curve representing an average of all the records for that particular set of conditions. The composite curves were then integrated to obtain the values of impulse and energy flux which are discussed below.

The composite curves are reproduced in Appendix III. The time scale is reduced by the cube root of the weight and each figure represents the results obtained at a given gauge position with all the charge sizes used. It will be noted that the curves diverge only in the region of the peak of the pulse, the remainder of the curve being virtually independent of charge size in most cases.

11.

A summary of the positive impulse values is given in Table XI.

Table XI

REDUCED POSITIVE IMPULSE: FIRST AND SECOND BUBBLE PULSES

Values apply for $W^{1/3}/R = 0.352$; R = distance from center of initial charge position. (No correction applied for bubble migration.)

Charge Weight (lb)	Depth (ft)	Reduced Positive Impulse, $I/W^{1/3}$ (lb sec/in. ² lb ^{1/3})									
		First Pulse					Second Pulse				
		G1	G2	G2,3	G3	G4	G1	G2	G2,3	G3	G4
0.505	250	1.39	---	1.34	---	1.32	0.66	---	0.51	---	0.46
2.507	250	1.43	---	1.33	---	1.22	0.71	---	0.57	---	0.47
0.505*	400	1.11	---	0.97	---	1.07	---	---	0.42	---	---
0.505	500	1.10	1.22	1.16	1.12	1.15	0.45	0.48	0.44	0.40	0.39
2.507	500	1.11	1.17	1.12	1.04	1.07	0.44	0.46	0.43	0.44	0.40
12.01	500	1.15	1.16	1.17	1.06	1.11	0.51	0.49	0.47	0.46	0.46

* Charges improperly boosted.

A composite pressure-time curve was drawn at each gauge position for a given charge size, and the values in Table XI were obtained by an integration under the positive phase of the curve, the impulse being defined by:

$$I = \int \Delta p \, dt$$

Since the impulse is very sensitive to slight base line error, the integrations were corrected in such a way that the net impulse over a complete pulse was equal to zero. A complete bubble pulse is defined by the interval between successive bubble maxima, and it is shown in Ref. (7) that the net impulse in this interval must be very nearly zero, i.e., the magnitudes of the positive and negative components of the impulse are nearly equal.

The a priori base lines selected on the basis of Appendix I are slightly in error, and as a result, integration of the composites led to results in which the positive and negative impulses differed. A slight shift of the base line (ca. 5 lb/in.²) sufficed in all cases to make the two components equal, and the resulting impulse values are the ones given in Table XI.

Impulses measured in the G1 position vertically above the charge are systematically high and those in the G4 position below the charge systematically low as would be expected on the basis of the migration results given in Table IX. As in the case of peak pressure (Table X) the impulse is higher off the cap end, and lower off the butt end, than off the cylindrical sides of the charge.

Using the G2,3 position off the cylindrical sides as being representative of the unperturbed impulse, it is seen that at each depth the impulse scales according to the ideal similarity law within the probable precision of measurement. (An exact statistical measure of the precision is not available because of the use of composite curves.)

This fact supports the qualitative indications of the composite curves that although the peak pressure is appreciably affected by migration, the remainder of the pressure-time curve is not.

It will be noted that the improperly boosted charges again give results which are significantly low.

12.

It is shown in Appendix I that to a first approximation the positive impulse would be expected to vary inversely as the sixth root of the absolute hydrostatic pressure at the point of detonation. A test of this prediction is given in Table XII.

Table XII

VARIATION OF POSITIVE IMPULSE WITH DEPTH OF DETONATION: FIRST BUBBLE PULSE

$$D_o = \text{Depth below surface} + 33 \text{ (ft)}$$

$$W^{1/3}/R = 0.352$$

D_o	$I/W^{1/3}$	$ID_o^{1/6}/W^{1/3}$
(ft)	(lb sec/in. ² lb ^{1/3})	
40	1.66*	3.1
283	1.34	3.4
533	1.15	3.3

* Value taken from Ref. (1), for rest position of 300 gm TNT charge near surface and corrected to $W^{1/3}/R = 0.352$. This value is probably low due to surface reflection cut-off in later stages of the pulse.

Since the quantity $ID_o^{1/6}/W^{1/3}$ is essentially constant with depth, the impulse is seen to vary approximately as the inverse sixth root of the hydrostatic pressure.

13.

The composite curves described above were also integrated to obtain the energy flux defined by:

$$F = \frac{1}{\rho_0 c_0} \int (\Delta p)^2 dt$$

where the integration is carried from the time of first bubble maximum to second bubble maximum for the first pulse and from the time of second bubble maximum to third bubble maximum for the second pulse. The time of first bubble maximum is defined as occurring at half the first period, etc.

The results of the energy flux integrations appear in Table XIII.

Table XIII

REDUCED ENERGY FLUX: FIRST AND SECOND BUBBLE PULSES

Values apply for $W^{1/3}R = 0.352$;
 R = distance from center of initial charge position (No correction applied for bubble migration.)

Charge Weight (lb)	Depth (ft)	Reduced Energy Flux; $F/W^{1/3}$ (in.lb/in. ² lb ^{1/3})									
		First Pulse					Second Pulse				
		G1	G2	G2,3	G3	G4	G1	G2	G2,3	G3	G4
0.505	250	161	---	141	---	122	23.2	----	15.0	----	11.1
2.507	250	154	---	125	---	101	28.4	----	16.4	----	11.1
0.505*	400	123	---	102	---	112	----	----	13.2	----	----
0.505	500	140	164	141	135	136	17.1	20.1	16.6	13.8	13.5
2.507	500	138	145	134	131	121	18.6	20.0	15.9	15.7	13.1
12.01	500	150	150	142	128	120	23.8	21.2	21.8	17.0	19.2

* Improperly boosted charges.

It is seen from Table XIII that the improperly boosted charges are again consistently low.

The energy flux at the cylindrical sides of the charge is appreciably affected by migration only in the most severe case, that of the 2.5 lb charges at 250 ft. Values off the cap and butt ends follow the pattern already established by the peak pressure and impulse results.

Since the energy flux depends upon the square of the pressure, it is not critically sensitive to small baseline uncertainties, and no correction was necessary as in the case of the impulse. The base line shift necessary to

correct the impulse was found to change the energy integral by less than 2%.

The energy flux in the second pulse of the 12 lb charges is unduly large and stems from the inconsistency in the peak pressure of this pulse which has previously been pointed out in Table IX.

A complete interpretation of the results of Table XIII with respect to total energy lost by the bubble and the overall energy partition in an underwater explosion is given in Ref. (7).

V. MEASUREMENT TECHNIQUES

14. Charges

The charges were cylinders of cast TNT and were boosted with pressed tetryl pellets. The tetryl was converted to an equivalent weight of TNT by multiplying by 1.03 as suggested by the results in Ref. (4). One gram was added to the charge weight to account for the explosive in the Engineer's Special Caps which were used to detonate the charges. The design and methods of making the charges are described in Ref. (8).

15. Piezoelectric Gauges

All the gauges used for these measurements were 7/8 in. diameter Type B tourmaline gauges described in Ref. (9). Average gauge sensitivity was approximately 25 micromicrocoulombs per lb/in.².

16. Rigging of Charge and Gauges.

Eight piezoelectric gauges were mounted on 3/16 in. steel cables in the plane of a 15 ft diameter steel ring, the charge being mounted at the center. Two gauges were mounted above, two below, and two off each side or end of the charge. A diagram of the arrangement is shown in Fig. 3.

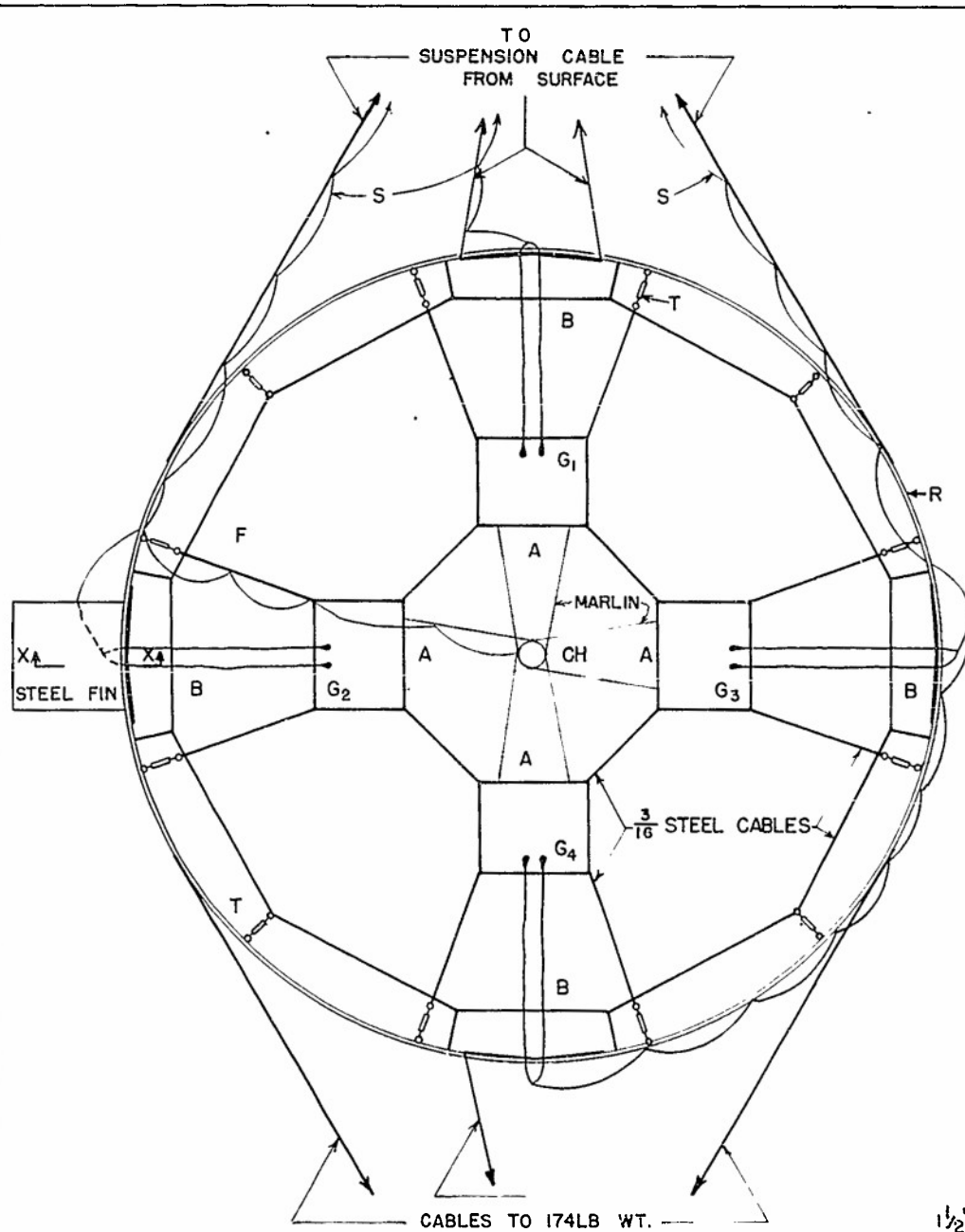
Gauges were arranged on the inner steel cable network for the 0.5 and 2.5 lb charges. This cable was removed, and the outer steel cable was used to position gauges for the 12 lb charges.

Charges were mounted so that the center of the charge was in the plane of the ring, and two charge orientations were used:

- i. axis of charge perpendicular to plane of ring
- ii. axis of charge horizontally oriented in plane of ring.

The following notation has been adopted to indicate gauge positions:

- G1: pair of gauges vertically above the charge
- G2: pair of gauges off cap end of charge when axis of charge is in the plane of the ring
- G3: pair of gauges off butt end of charge opposite G2



LEGEND

- A - GAUGE POSITIONS FOR 1/2 LB CHARGES
- B - GAUGE POSITIONS FOR 12 LB CHARGES (INNER STEEL CABLE NETWORK REMOVED)
- G - GAUGE POSITIONS FOR 2.5 LB CHARGES
- CH - CHARGE
- F - FIRING LINE
- S - SIMPLEX FO 5789 CABLES
- T - TURNBUCKLES
- R - 15 FT DIA. STEEL RING (1 1/2 IN. DIA SOLID STOCK)

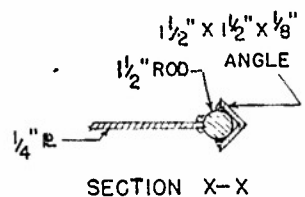


FIG. 3
 RIG FOR FREE WATER BUBBLE SERIES
 UERL WOODS HOLE, MASS.

G2,3: two pairs of gauges, each pair horizontally off cylindrical sides of charge when charge axis is perpendicular to plane of ring.

G4: pair of gauges vertically below charge.

Dimensions were so chosen that the wire structure did not come in contact with the bubble at its maximum expansion and the $3/16$ in. cables were never damaged or appreciably loosened by the forces of the explosion. Four $1\frac{1}{2}$ in. angle irons $2\frac{1}{2}$ ft long were welded to the inside of the ring behind each pair of gauges in an effort to minimize direct shock wave reflection from the ring.

To prevent rotation of the ring and consequent twisting of the electrical cables, a steel plate 2 ft x 2 ft x $\frac{1}{4}$ in. was welded on the outside of the ring as shown in Fig. 3. Guy wires above and below the ring were used to minimize tilting. The ring was lowered over the side of the vessel by means of a boom and a $3/8$ in. steel suspension cable.

17. Depth Measurements

The overall depth of water was measured by a fathometer which was occasionally checked by a hand sounding line. All experiments were performed in such depths that the charge was always at least 150 ft. away from the bottom.

The depth of the charge was determined by the measured length of the suspension cable. This method was very reliable because experiments were performed in a region of negligible tidal currents, and the suspension always hung vertically downward. This is confirmed by the reproducibility of the period measurements tabulated in Chapter II. As a further precaution depths were also checked by means of a depth gauge of the type described in Ref. (10), and these measurements were always in good agreement with the length of suspension cable.

18. Electrical Cables

Continuous 600 ft lengths of Simplex (F.C. 5789) signal-free co-axial cable were used between the gauges and oscilloscopes, thus avoiding occurrence of cable signal for an interval sufficiently long to allow faithful recording of the first two bubble pulses. Cable signal effects were further minimized by the relatively high sensitivity of the gauges. The polyethylene core of the Simplex cable also served to render negligible any low frequency distortion due to dielectric dispersion.

The Simplex cables led from the gauges directly to the vessel, where they terminated in compensating networks in the master control panel. Double-ended compensation was not feasible because of possible cable signal arising from cable discontinuities and possible damage to the remote compensating networks which would have had to be placed relatively close to the charge. However, single-ended compensation¹¹⁾ was introduced mainly to reduce the amplitude of a series of voltage maxima characteristic of open circuit resonance occurring at frequencies above 100 kc. With termination, the response was flat within 1.2% from 50 cps to 100 kc and dropped off rapidly at higher frequencies. The terminator comprised a series R-C network, with the resistance $R = 95$ ohms (1.5 times the surge impedance of the cable) and the capacitance $C = 31,000 \mu\mu f$

(approximately twice the total cable capacity). It should be noted that compensation, in general, is not critical for such a long-duration phenomenon as the bubble pulse.

19. Recording Instruments

The recording apparatus consisted of the eight channel setup of the schooner "Reliance"¹²). In order to avoid low frequency distortion, it was necessary to increase the input impedance by using cathode follower preamplifiers. The final overall time constant of the recording circuits was about 500 millisecc.

A 110 volt DC motor with variable armature voltage was used to drive the rotating drum cameras. Writing speeds were thus varied from 125 to 400 millisecc per revolution of the 10 in. circumference drums.

VI. SUMMARY AND CONCLUSIONS

The results tabulated in preceding chapters have indicated:

(i) That the peak pressure of the first bubble pulse is exceedingly sensitive to migration effects — much more so than theoretically predicted. Therefore, the peak pressure of the pulse does not scale ideally with the charge size even at great depths where the migrations are small.

(ii) The positive impulse is virtually unaffected by small migrations and scales properly under circumstances where the peak pressure scaling fails.

(iii) The energy flux is also relatively insensitive to migration effects and scales according to the ideal scaling law when the migration is small.

(iv) The period of the first pulse shows a slight but significant departure from cube-root scaling with charge size, although the reality of this effect is somewhat in doubt because of uncertainty as to the effect of the presence of the relatively large amount of tetryl booster in the 0.5 lb charges.

(v) A significant orientation effect appears to exist, the asymmetry being greater in the case of the smaller charges. This effect consists of higher values of peak pressure, impulse, etc., off the cap end and lower values off the butt end than are obtained off the cylindrical sides of the charge.

In view of the results obtained and experience acquired in this series of experiments, it is felt that a certain amount of additional investigation is desirable in order to establish the following points or resolve the following uncertainties:

(i) The cause of the observed slight failure of scaling of period with charge size.

(ii) The characteristics of the observed orientation effect with respect to variation of charge size, shape, type of explosive, etc.

(iii) More detailed information concerning the quantitative effect of migration on peak pressure, impulse, and energy flux.

(iv) A study of the variation of the peak pressure of the first pulse with distance from the charge. (It is commonly assumed that the wave is very nearly acoustic and the amplitude varies inversely as the distance. No direct check of this assumption has yet been made with instruments capable of the precision attained in experiments described in this report.) If the rate of decay of pressure were to be found to be significantly more rapid than the inverse first power, the result would account at least for some part of the energy which is lost between the first and second bubble maxima but is not observed as compressional energy in the acoustic radiation. (See Ref. 7.)

(v) In the present series of experiments, the gain of the amplifiers was set so as to record the first pulse with optimum amplitude. At first, a gain-changing device was introduced in such a way that the signal produced by the passage of the shock was attenuated to about the same amplitude as the first pulse, and then relays were opened to allow recording of the pulse at the proper gain setting. The opening of the relays was found to introduce signals which caused fairly large displacement of the base line. Because of this, the gain changer was eliminated, and the full signal produced by passage of the shock wave was applied to the amplifiers. This technique proved to be adequate, in that the amplifiers were not seriously overloaded and the base line uncertainty was relatively small. Final critical examination of the records, however, indicates that the baseline was slightly but systematically shifted (by about 30 lb/in.²) in the negative direction. This was probably due to the drawing of grid current by the high amplitude shock-wave signal. In future experiments it would be desirable to eliminate this difficulty by introducing a voltage limiting circuit that will not allow passage of the excessively high signal and will prevent the above grid current effects.

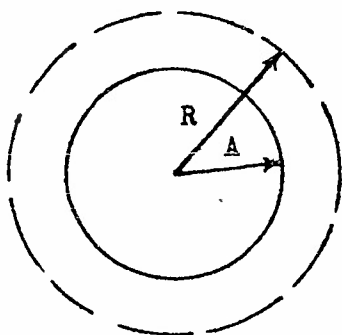
Provision of an undisturbed base line would allow a more objective measurement of the low amplitude portions of the bubble pulse (i.e., negative phase; time of occurrence of zero pressure points, positive impulse, etc.) than was available in this series.

APPENDIX I

THE PULSATING STATIONARY GAS GLOBE

(Incompressive Approximation)

A. The Energy Equation



Consider a sphere of radius A expanding with radial velocity A' . The volume rate of displacement of fluid at the periphery of the sphere is given by:

$$4\pi A^2 A' \quad (A-1)$$

Similarly, the volume rate of displacement at R is given by:

$$4\pi R^2 R' \quad (A-2)$$

If the fluid is assumed to be incompressive, Eqs. (A-1) and (A-2) may be equated directly, giving:

$$A^2 A' = R^2 R' \quad (A-3)$$

The kinetic energy of the fluid external to radius A is given by

$$J = \int_A^{\infty} 4\pi R^2 \left(\frac{\rho R'^2}{2} \right) dR = 2\pi\rho A^4 A'^2 \int_A^{\infty} \frac{dR}{R^2} \quad (A-4)$$

Integration of Eq. (A-4) gives:

$$J = 2\pi\rho A^3 A'^2 \quad (A-5)$$

The potential energy of the system is:

$$U = \frac{4}{3}\pi A^3 P_0 + G(A) \quad (A-6)$$

where the first term represents energy stored against hydrostatic pressure (P_0 being the absolute hydrostatic pressure at the depth of the bubble center), and the second term represents the internal energy of the gas in the bubble. The zero of internal energy is defined as the infinite limit of adiabatic expansion, thus:

$$G(A) = \int_A^{\infty} p dV \quad (A-7)$$

where the line integral is taken along an adiabat, and V represents the total volume of gas.

If it is assumed that the gas approximates ideal behavior:

$$p v^{\gamma} = \text{const.} = k_1$$

where v is specific volume, and in general:

$$p = \frac{k_1 M^{\gamma}}{V^{\gamma}} \quad (A-8)$$

where M is the mass of gas, and γ is the ratio of heat capacities.

Then:

$$G(A) = k_1 M^{\gamma} \int_{V_A}^{\infty} \frac{dV}{V^{\gamma}} \frac{k_1 M^{\gamma}}{(\gamma-1) A^{3(\gamma-1)} \left(\frac{4\pi}{3}\right)^{\gamma-1}} \quad (A-8a)$$

If the total energy associated with the oscillation is denoted by E , the energy equation becomes:

$$2 \pi \rho A^3 A'^2 + \frac{4}{3} \pi A^3 P_0 + G(A) = E \quad (A-9)$$

Following Shiffman and Friedman⁵⁾ it is convenient to transform to dimensionless variables by using the following scale factors for length and time respectively:

$$L = \left(\frac{3E}{4\pi P_0}\right)^{1/3} \quad (A-10)$$

$$C = L \left(\frac{3\rho}{2P_0}\right)^{1/2} \quad (A-11)$$

Combining Eqs. (A-9), (A-10), (A-11):

$$a^3 \dot{a}^2 + a^3 + \frac{k}{a^3(\gamma-1)} = 1 \quad (\text{A-12})$$

where $a = \frac{A}{L}$, the dot denotes derivative with respect to non-dimensional time, and L

$$k = \frac{k_1 P_0 \gamma^{-1}}{(\gamma-1) \mathcal{E}^\gamma} \quad (\text{A-13})$$

\mathcal{E} being the bubble energy per unit mass of gas (or explosive charge).

Since the bubble is at maximum or minimum when $\dot{a} = 0$, the maximum and minimum bubble radii are given in Eq. (A-12) by the roots of the equation:

$$a^3 + \frac{k}{a^3(\gamma-1)} - 1 = 0 \quad (\text{A-14})$$

B. The Pressure at Bubble Minimum

Assuming the existence of a velocity potential Φ defined by:

$$R' = - \frac{\partial \Phi}{\partial R}$$

and combining with Eq. (A-3):

$$\Phi = \frac{A^2 A'}{R} \quad (\text{A-15})$$

where Φ is set equal to zero at infinite values of R .

Bernoulli's equation gives the excess pressure in the fluid in terms of the velocity potential:

$$\frac{\Delta p}{\rho} = \frac{\partial \Phi}{\partial T} - \frac{1}{2} (\nabla \Phi)^2 \quad (\text{A-16})$$

(the partial derivative being taken with respect to dimensional time, T).

The second term is negligibly small compared to the first. Using Eq. (A-15):

$$\Delta p \cong \frac{\rho(A^2 \dot{a}^2)}{R} = \frac{\rho L^3}{C^2 R} (a^2 \ddot{a})^* \quad (\text{A-17})$$

An expression for $(a^2 \ddot{a})^*$ can be obtained from the equations of motion. The most convenient method is to apply the Lagrangian equation to the energy expression.

$$\frac{d}{dt} \left(\frac{\partial \mathcal{L}}{\partial \dot{a}} \right) - \frac{\partial \mathcal{L}}{\partial a} = 0 \quad (\text{A-18})$$

where $\mathcal{L} = J - U$ and t is the non-dimensional time.

From Eq. (A-12):

$$\mathcal{L} = a^3 \dot{a}^2 - a^3 - \frac{k}{a^{3(\gamma-1)}} \quad (\text{A-19})$$

Combining Eqs. (A-18) and (A-19):

$$(a^2 \ddot{a})^* = \frac{a \dot{a}^2}{2} - \frac{3a}{2} + \frac{3(\gamma-1)k}{2a^{3\gamma-1}} \quad (\text{A-20})$$

Combining Eqs. (A-20), (A-17), (A-10), and (A-11):

$$\Delta p = \frac{2P_0 L}{3R} \left[\frac{a \dot{a}^2}{2} - \frac{3a}{2} + \frac{3(\gamma-1)k}{2a^{3\gamma-1}} \right] \quad (\text{A-21})$$

When a is at a maximum or minimum $\dot{a} = 0$, and:

$$\Delta p_M = - \frac{P_0 L}{R} \left[a_M - \frac{(\gamma-1)k}{a_M^{3\gamma-1}} \right] \quad (\text{A-22})$$

Since the incompressive approximation should be quite accurate in the neighborhood of the bubble maximum (when the pressures are very low), Eq. (A-22) should be an equally accurate representation of the pressure in the fluid when the bubble is at maximum radius.

It will be noted that since γ is of the order of 1.3, k of the order of 0.2, and a_M about 0.9, the first term in the bracket of Eq. (A-22) dominates, the second term representing a relatively small correction for the internal energy of the gas, depending upon the adiabatic equation of

state parameters k_1 and γ . Thus the minimum pressure is negative relative to the original hydrostatic level, as would be expected, and is not critically dependent upon the equation of state of the gas.

Since a_M represents the non-dimensional maximum bubble radius and L is the scale factor of length, the first term in Eq. (A-22) represents the pressure below hydrostatic which would be observed at a distance R from a bubble of maximum radius $L a_M$ having an absolute internal pressure of zero. The second term in the equation corrects for the actual internal pressure of the gas.

Adopting a bubble energy of 470 cal. per gram of explosive

$$L = 13.5 \left(\frac{W}{D_0} \right)^{1/3} \quad (A-23)$$

where W is the charge weight in lb and D_0 is absolute hydrostatic depth in ft (i.e., depth below the surface plus 33 ft).

Rewriting Eq. (A-22)

$$\Delta P_M = - 6.01 D_0^{2/3} \frac{W^{1/3}}{R} \left[a_M - \frac{(\gamma - 1)k}{a_M^{3\gamma - 1}} \right] \quad (A-24)$$

where ΔP_M is in lb/in.² and R is in ft.

Using the results of Ref. (4) for 1/2 lb TNT charges at 300 to 500 ft, the measured maximum radius A_M is given empirically by:

$$A_M = 12.6 \left(\frac{W}{D_0} \right)^{1/3} \quad (A-25)$$

and consequently $a_M = 0.93$.

The internal energy correction term depends upon the selection of the equation of state parameters, and various aspects of this problem are discussed in Ref. (4). For the present purpose, it is sufficient to select rough average values:

$$\left. \begin{array}{l} (\gamma - 1) \cong 0.3 \\ k \cong 0.2 \\ a_M^{3\gamma - 1} \cong 0.85 \end{array} \right\} \quad (A-26)$$

Combining Eqs. (A-24), (A-25), and (A-26):

$$\Delta P_M = - 5.16 D_0^{2/3} \frac{W^{1/3}}{R} \quad (A-27)$$

Results obtained from Eq. (A-27) are given in Table A-I below:

Table A-I.

NEGATIVE PRESSURE AT BUBBLE MAXIMUM FOR VARIOUS CHARGE DEPTHS

$$W^{1/3}/R = 0.352$$

D_0 (ft)	Δp_M (lb/in. ²)
283	-78
433	-105
533	-120

As the bubble collapses, and a approaches its minimum value (i.e., Δp approaches a maximum), it is seen from Eq. (A-22) that the second term in the bracket becomes the dominant term and Δp becomes positive. Thus the peak pressure of the bubble pulse depends critically on k_1 and γ , but in addition to the fact that neither of these parameters is accurately known, there is also no reason to believe that the ideal gas adiabatic (Eq. A-8) continues to be an adequate approximation under the high pressures and temperatures attained in the neighborhood of the bubble minimum. Furthermore, Eq. (A-22), which is based on the assumption of incompressibility of the surrounding fluid, becomes less and less accurate as increasing pressure makes more pronounced the radiative effects of acoustic compressibility.

Dependence of Positive Impulse on Depth. Impulse is defined by:

$$I = \int \Delta p \, dT = C \int \Delta p \, dt \quad (A-28)$$

where T and t are dimensional and non-dimensional time respectively.

Combining Eqs. (A-17) and (A-28):

$$\begin{aligned} I &= \frac{\rho L^3}{OR} \int (a^2 \dot{a}) \, dt \\ &= \frac{2 \rho_0 L G}{3R} \int d(a^2 \dot{a}) \end{aligned} \quad (A-29)$$

If the positive impulse is desired, the integral must be evaluated between the limits at which $(a^2 \dot{a})$ is successively zero, i.e., between successive maxima of the integrand $a^2 \dot{a}$. The value of the integral is

approximately 1.1, being very insensitive to changes in k.

The dependence of the positive impulse on depth can therefore be obtained (to a first approximation) directly from the coefficient before the integral in Eq. (A-29). Since L and C vary inversely as the 1/3 and 5/6 powers of P_0 respectively, it is seen that the impulse varies inversely as the 1/6 power of the hydrostatic pressure.

APPENDIX II

TABULATION OF ORIGINAL DATA

The following tables show peak pressure values for first and second bubble pulses obtained in various gauge positions around the charge.

Position G1: gauges vertically above charge
G2: gauges horizontally off cap end of charge
G2,3: gauges horizontally off cylindrical sides of charge
G3: gauges horizontally off butt end of charge
G4: gauges vertically below charge

Each number represents the average of two gauge readings except in a few cases where one gauge of the pair failed. The values for the G2,3 position represent the average of four gauge readings.

σ_m represents the standard deviation of the mean.

R represents distance of each pair of gauges from center of initial charge position.

Baseline with respect to which the peak pressure is measured was adjusted in accordance with the theory developed in Appendix I.

Table A-II

FIRST AND SECOND BUBBLE PULSE PEAK PRESSURES

W = 0.505 lb TNT
 R = 2.25 ft
 Depth 250 ft

Baseline adjusted to -80 lb/in.² at first bubble maximum

Shot Number	Peak Pressures (lb/in. ²)					
	First Pulse			Second Pulse		
	G1	G2,3	G4	G1	G2,3	G4
734	1310	1140	995	285	230	180
735	1280	1110	955	285	225	180
736	1330	1140	965	300	220	180
737	1240	1080	935	280	205	190
Avg	1290	1120	960	290	220	185
σ_m	20	14	12	5	5	3

Table A-III

FIRST AND SECOND BUBBLE PULSE PEAK PRESSURES

W = 2.507 lb TNT
 R = 3.84 ft
 Depth 250 ft

Baseline adjusted to -80 lb/in.² at first bubble maximum

Shot Number	Peak Pressures (lb/in. ²)					
	First Pulse			Second Pulse		
	G1	G2,3	G4	G1	G2,3	G4
738	1265	1000	820	290	205	150
739	1270	1010	840	295	215	170
Avg.	1270	1005	830	290	210	160

Table A-IV

FIRST AND SECOND BUBBLE PULSE PEAK PRESSURES

W = 0.505 lb TNT

R = 2.25 ft

Depth 500 ft

Baseline adjusted to -120 lb/in.^2 at first bubble maximum

Shot Number	Peak Pressures (lb/in. ²)									
	First Pulse					Second Pulse				
	G1	G2	G2,3	G3	G4	G1	G2	G2,3	G3	G4
713	1165	----	1230	----	1170	260	---	275	---	260
714	1230	----	1210	----	----	240	---	255	---	---
716	1260	1340	----	1085	----	270	295	---	230	---
717	1270	1440	----	1140	----	250	290	---	240	---
729	1280	----	1200	----	1160	275	---	255	---	235
730	1250	1365	----	1100	1150	255	290	---	230	225
731	1255	----	1210	----	1130	260	---	255	---	230
732	1265	1310	----	1050	1120	270	270	---	225	225
Avg	1260*	1365	1210	1095	1145	260	285	260	230	235
σ_m	5	19	6	21	9	4	2	5	3	6

* Omitting Shot 713

Table A-V

FIRST AND SECOND BUBBLE PULSE PEAK PRESSURES

W = 2.507 lb TNT

R = 3.84 ft

Depth 500 ft

Baseline adjusted to -120 lb/in.^2 at first bubble maximum

Shot Number	Peak Pressure (lb/in. ²)									
	First Pulse					Second Pulse				
	G1	G2	G2,3	G3	G4	G1	G2	G2,3	G3	G4
701	1260	----	1160	----	1090	290	---	245	---	220
702	1260	1160	----	1120	1080	310	280	---	230	220
709	1130	----	1200	----	1075	260	---	260	---	220
710	1250	1270	----	1200	1075	290	300	---	250	235
711	1270	----	1200	----	1060	280	---	280	---	230
712	1245	1225	----	1160	----	270	295	---	250	---
725	1275	----	1155	----	1030	255	---	245	---	200
726	1250	1175	----	1120	1105	280	280	---	250	240
727	1310	----	1160	----	1060	270	---	230	---	200
728	1285	1200	----	1160	1080	275	280	---	240	230
740	1250	----	1140	----	1050	245	---	240	---	210
741	1220	1170	----	1140	1045	260	240	---	220	185
Avg	1250	1200	1170	1150	1070	275	280	250	240	215
σ_m	10	17	10	12	7	5	9	7	5	5

Table A-VI

FIRST AND SECOND BUBBLE PULSE PEAK PRESSURES

W = 12.01 lb TNT

R = 6.50 ft

Depth 500 ft

Baseline adjusted to -120 lb/in.^2 at first bubble maximum

Shot Number	Peak Pressures (lb/in. ²)									
	First Pulse					Second Pulse				
	G1	G2	G2,3	G3	G4	G1	G2	G2,3	G3	G4
703	1250	----	----	1080	1000	270	---	---	235	230
706	1255	----	1110	----	950	290	---	250	---	245
707	1290	----	1180	----	1000	320	---	295	---	255
708	1310	1240	----	1105	1005	285	300	---	240	235
718	1300	----	1135	----	----	295	---	270	---	----
720	1280	1190	----	1095	----	325	295	---	260	----
721	1250	----	1180	----	----	320	---	270	---	----
722	1320	1185	----	1135	1035	310	290	---	265	235
723	1330	----	1170	----	980	310	---	275	---	255
724	1325	1195	----	1180	1055	275	---	---	255	235
742	1320	----	1110	----	960	300	---	245	---	215
743	1330	----	1145	----	960	310	---	250	---	200
Avg	1300	1200	1145	1120	995	300	295	265	250	235
σ_m	9	13	12	20	12	5	3	7	6	6

Table A-VII

FIRST AND SECOND BUBBLE PULSE PEAK PRESSURES

W = 0.505 lb TNT*

R = 2.25 ft

Depth 400 ft

Baseline adjusted to -105 lb/in.^2 at first bubble maximum

Shot Number	Peak Pressures (lb/in. ²)					
	First Pulse			Second Pulse		
	G1	G2,3	G4	G1	G2,3	G4
698	1140	1020	990	260	215	190
699	1130	1000	990	270	215	180
Avg	1135	1010	990	265	215	185

* Charges improperly boosted.

APPENDIX III
COMPOSITE CURVES

Figures A-1 thru A-8 represent composite pressure-time curves for various gauge positions. The curves were obtained by means of the procedure described in Section 10.

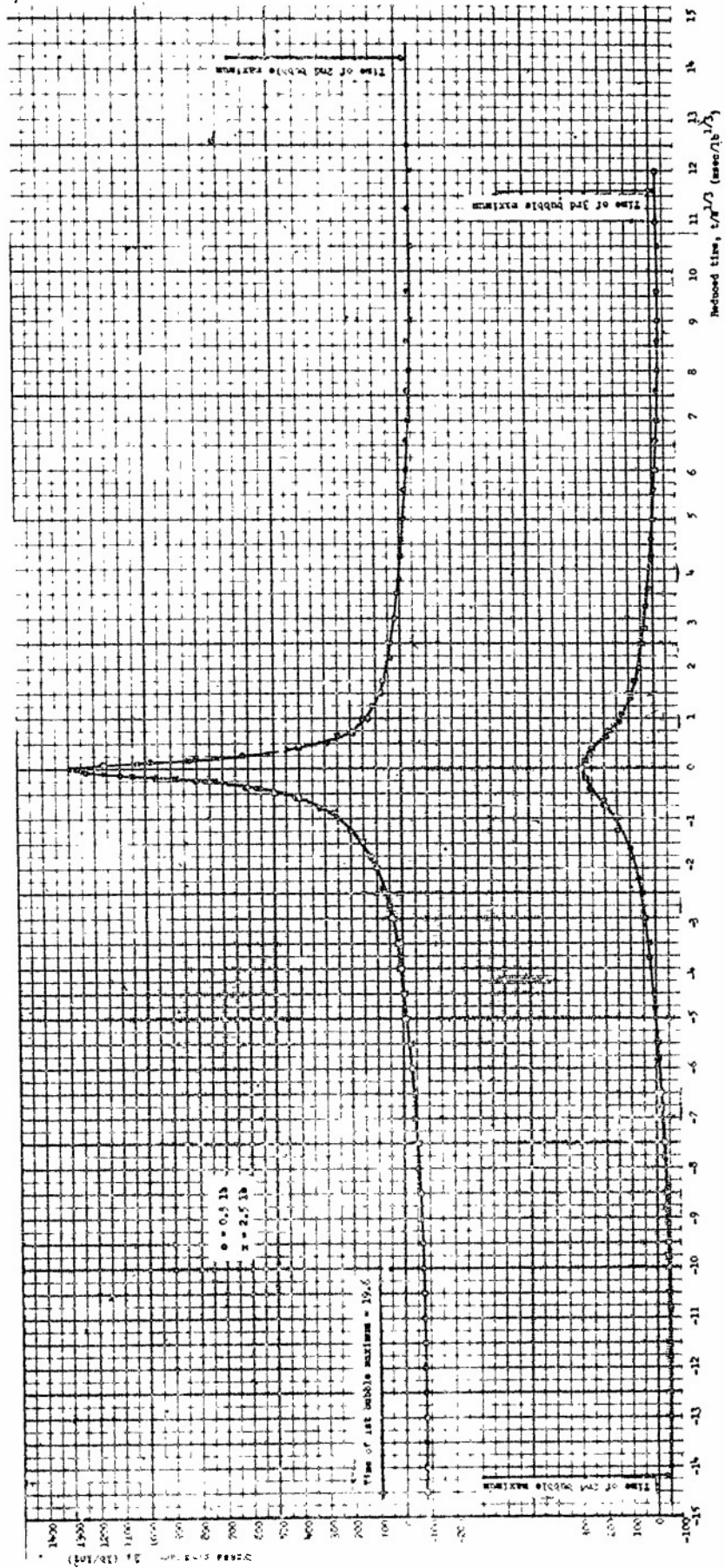


FIG. 4-1

Composite bubble pulse curves: pressure vs. time

For $W/R = 0.2$, charge depth 850 ft, gauge position 0-1.

W = charge weight (lb)
 R = distance of gauge from center of
 initial charge position (ft)

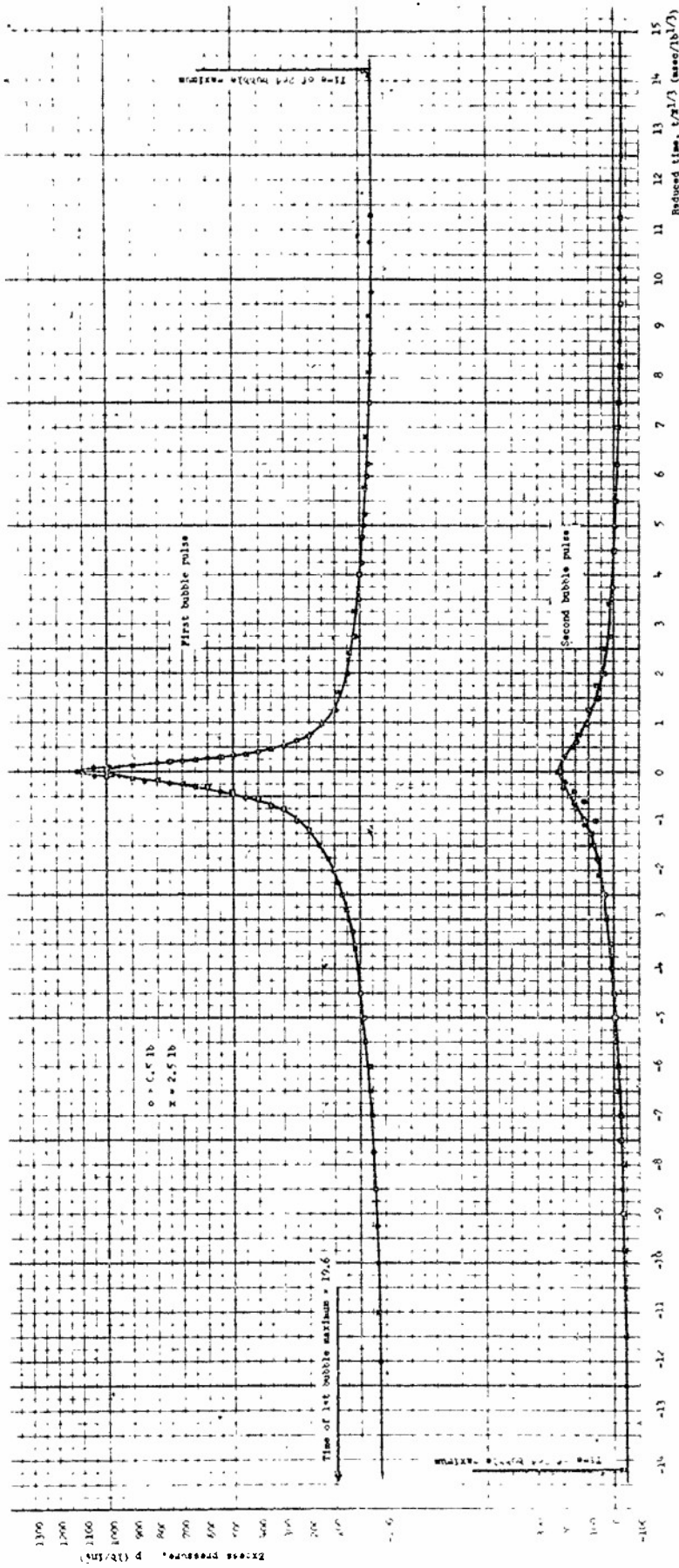


FIG. A-8
 Composite bubble pulse curves: pressure vs. time
 for $W/x/R = 0.258$, charge depth 120 ft, gauge position 0-5, 2.

W = charge weight (lb)
 x = distance of gauge from center of
 initial charge position (ft)

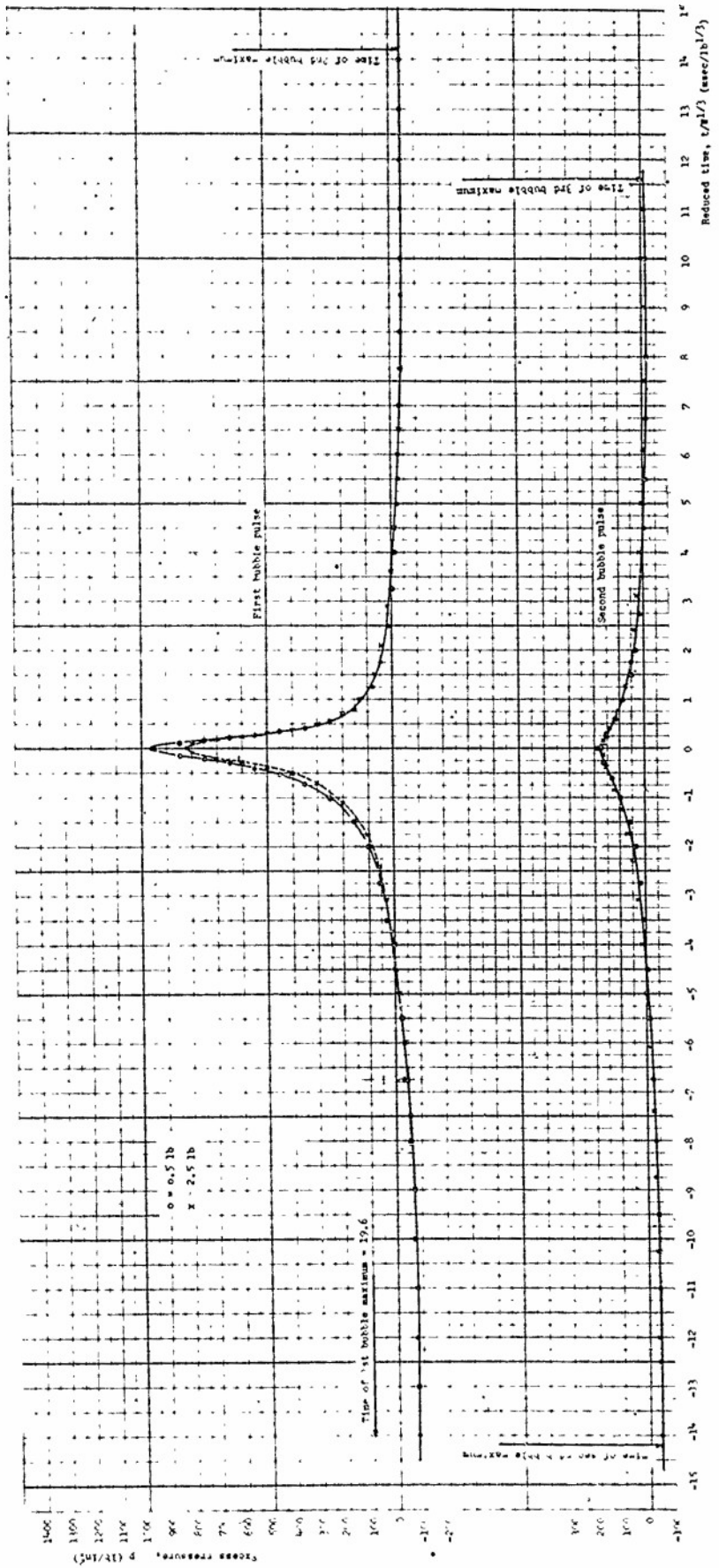


Fig. 4-3

Composite bubble pulse curves: pressure vs. time

for $g/H^2/R = 0.252$, charge depth 250 ft, gauge position 0-4.

m = charge weight (lb)
 H = distance of gauge from center of initial charge position (ft)

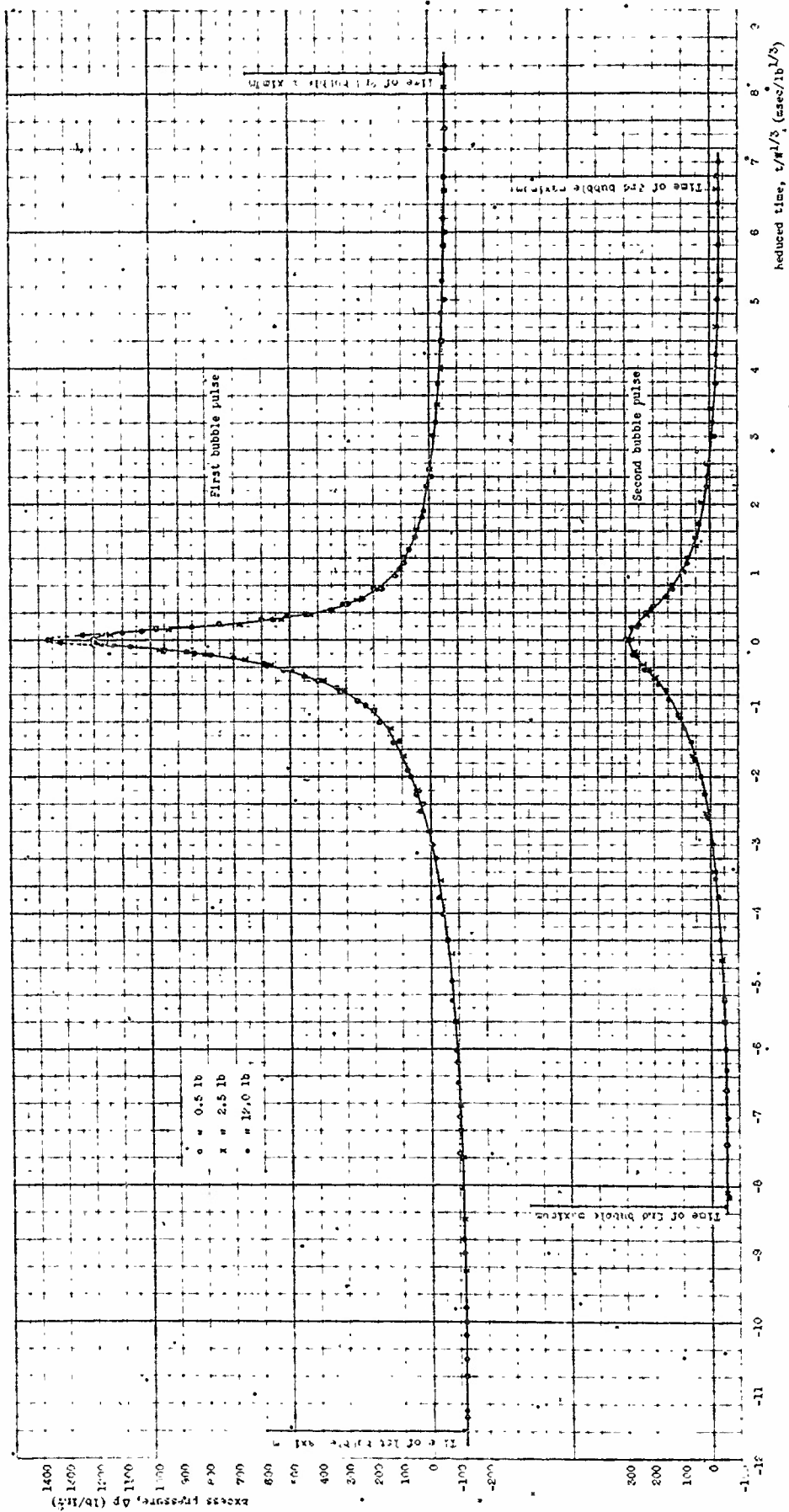


Fig. A-5
 Composite bubble pulse curves: pressure vs. time
 for $\mu^{1/3}/k = 0.352$, charge depth 500 ft, gauge position G-2.

W = charge weight (lb)
 k = distance of gauge from center of
 initial charge position (ft)

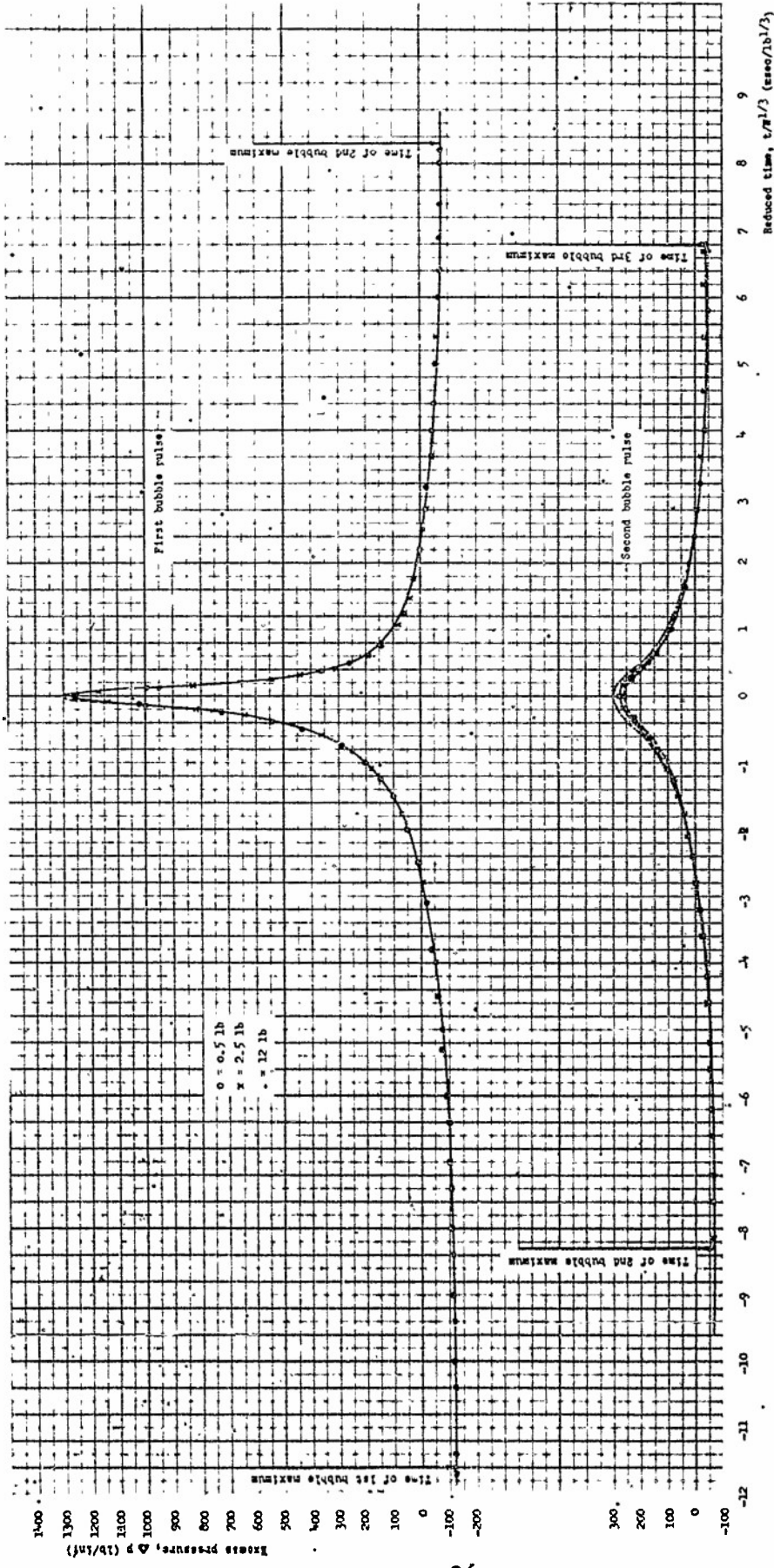


Fig. A-4

Composite bubble pulse curves: pressure vs. time
 for $W/S/R = 0.358$, charge depth 500 ft, gauge position G-1.

- W = charge weight (lb)
- X = distance of gauge from center of
- R = initial charge position (ft)

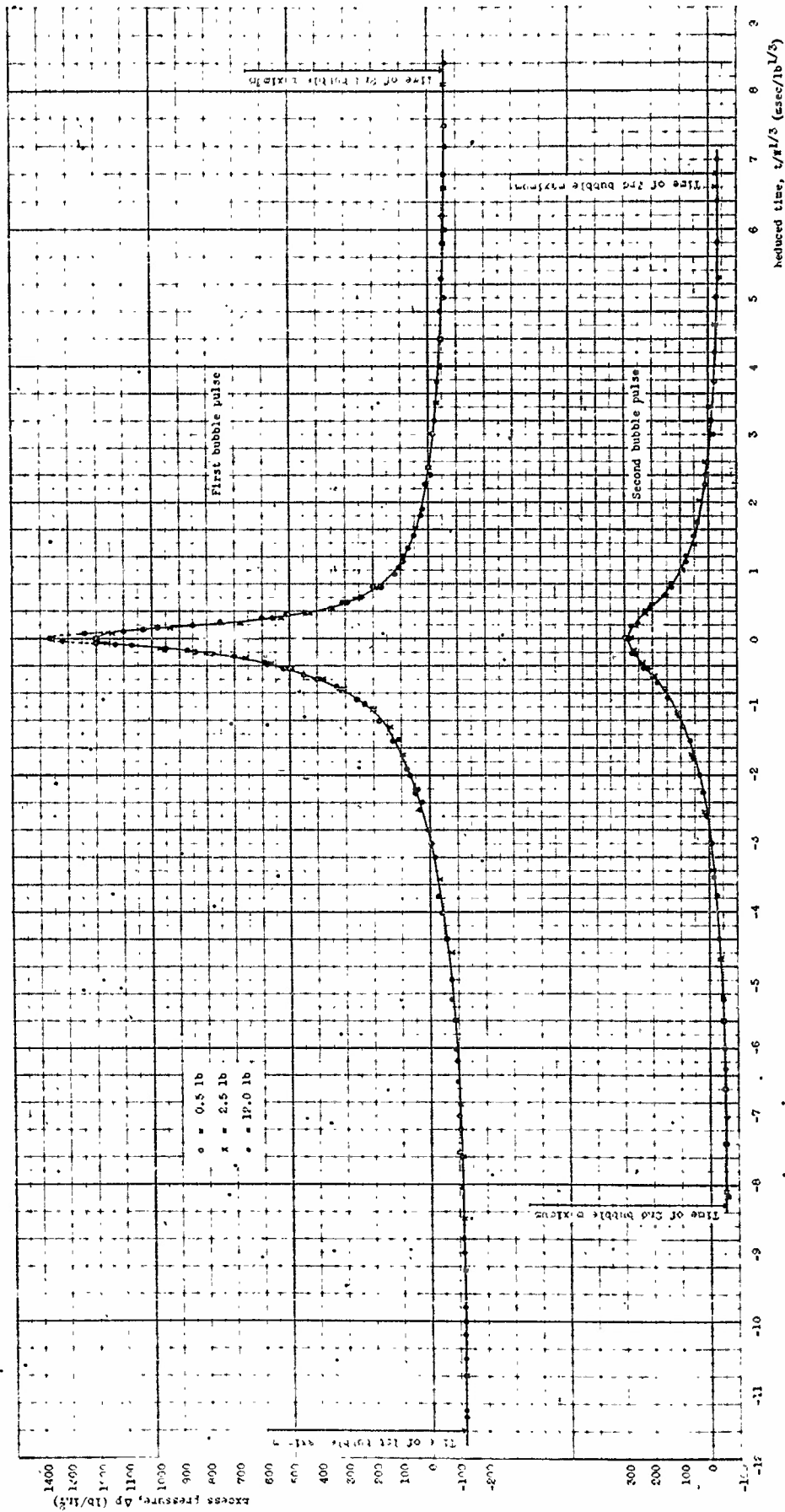


Fig. A-5
 Composite bubble pulse curves: pressure vs. time
 for $\mu/\rho = 0.252$, charge depth 500 ft, gauge position G-2.

W = charge weight (lb)
 x = distance of gauge from center of
 initial charge position (ft)

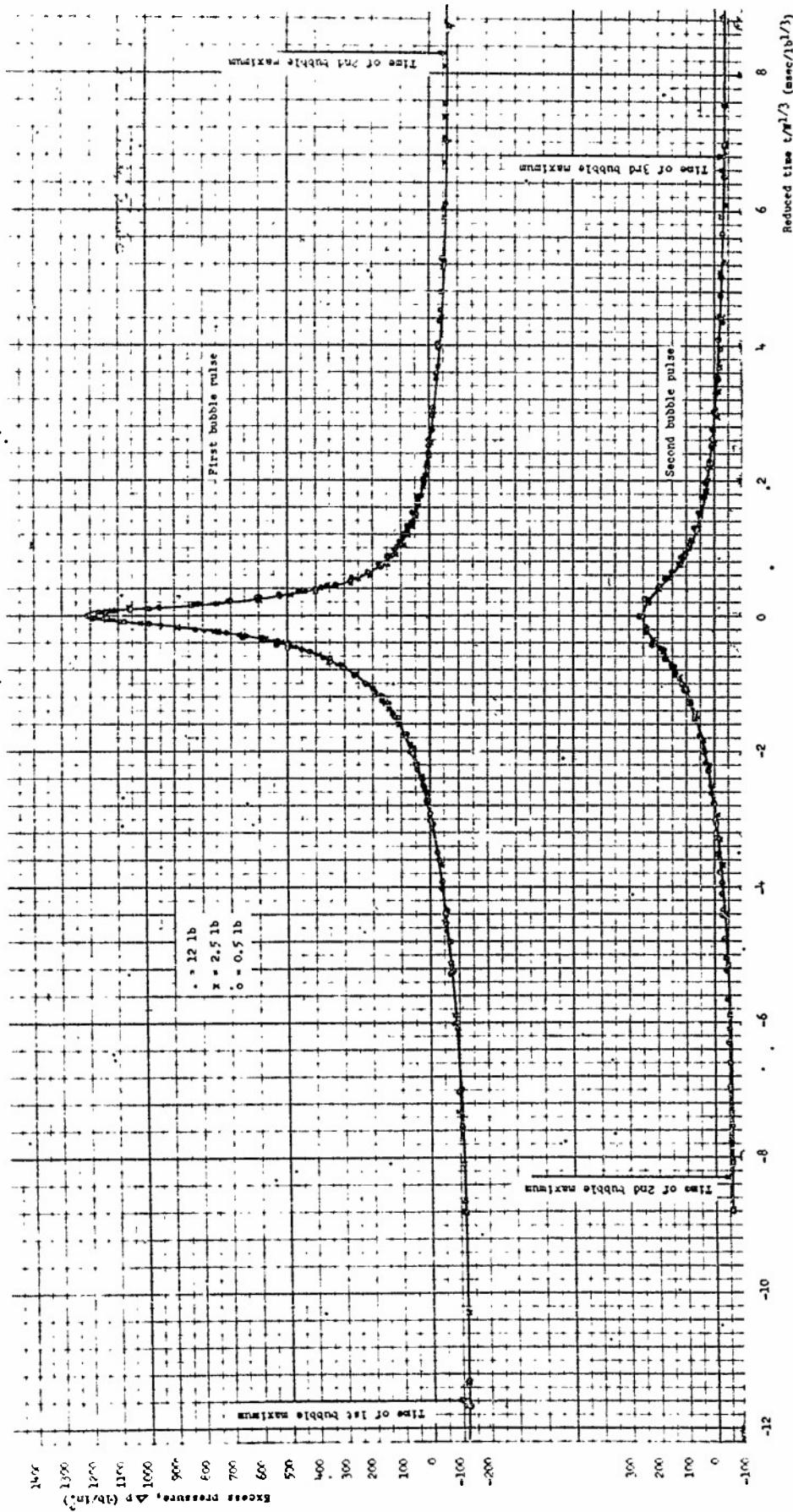


Fig. A-8

Composite bubble pulse curves: pressure vs. time
 for $\mu^{1/2}/R = 0.358$, charge depth 500 ft, gauge position 5-9,3.

W = charge weight (lb)
 R = distance of gauge from center of
 initial charge position (ft)

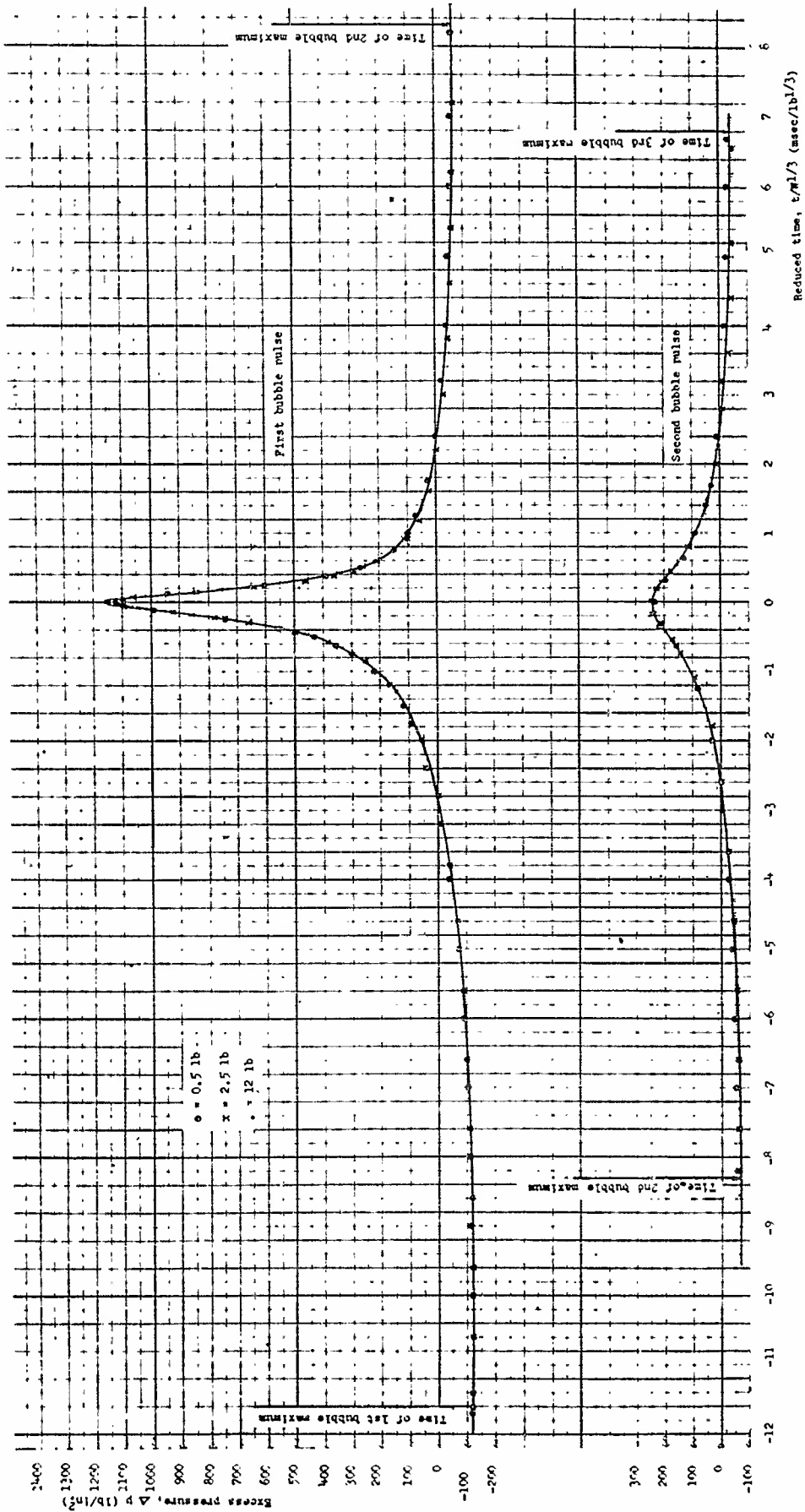


Fig. A-7

Composite bubble pulse curves: pressure vs. time
 for $w^{1/3}/H = 0.252$, charge depth 500 ft, gauge position 0-3.

w = charge weight (lb)
 H = distance of gauge from center of
 initial charge position (ft)

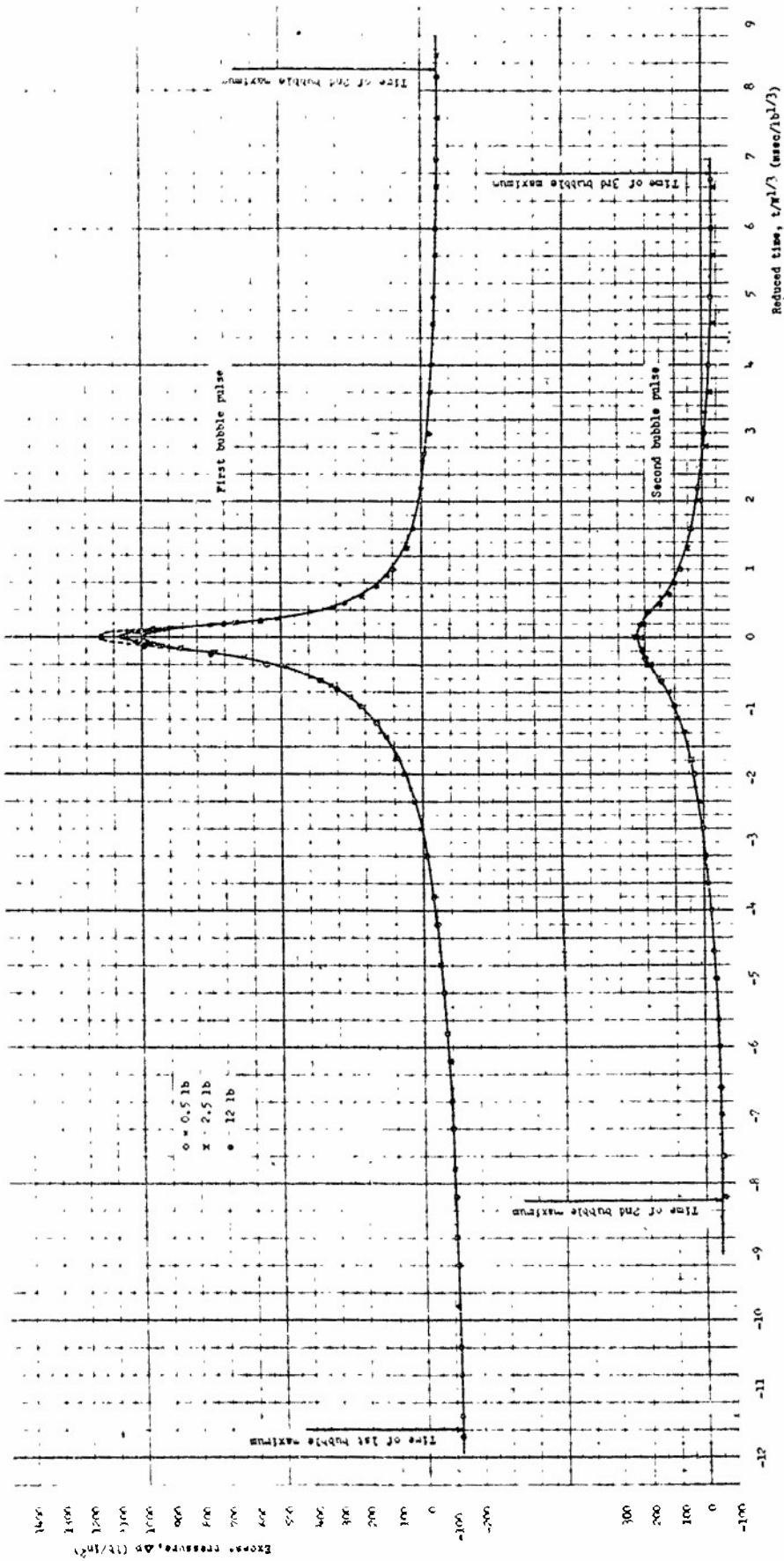


Fig. A-8

Composite bubble pulse curves: pressure vs. time
 for $a^2/2R = 0.252$, charge depth 500 ft, gauge position G-4.

A = charge weight (lb)
 R = distance of gauge from center of
 initial charge position (ft)

LIST OF REFERENCES

1. OSRD 6578, NDRC A-470.
2. OSRD 6242, NDRC A-364.
3. NavOrd 409.
4. Measurement of Bubble Pulse Phenomena III: Radius and Period Studies, by J. C. Decius, E. Swift, Jr., NavOrd 97-46.
5. Studies on the Gas Bubble Resulting from Underwater Explosions: On the Best Location of a Mine Near the Sea Bed, by M. Shiffman and B. Friedman, Applied Mathematics Panel NDRC, AMP Report 37.1R, AMG-NYU No. 49, May 1944.
6. Undex 10.
7. Energy Partition in Underwater Explosion Phenomena, by A. B. Arons and D. R. Yennie, NavOrd 406.
8. OSRD 6259, NDRC A-381.
9. OSRD 6239, NDRC A-361.
10. NavOrd 404.
11. The Use of Electrical Cables with Piezoelectric Gauges, by R. H. Cole, OSRD 4561, NDRC A-306, Jan. 1945.
12. OSRD 6240, NDRC A-362.

Reproduced by



CENTRAL AIR DOCUMENTS OFFICE

WRIGHT-PATTERSON AIR FORCE BASE - DAYTON, OHIO

REEL-6

2 7 2 9 B

A. T. I

5 8 4 1 7

The
U.S. GOVERNMENT

IS ABSOLVED

FROM ANY LITIGATION WHICH MAY ENSUE FROM ANY
INFRINGEMENT ON DOMESTIC OR FOREIGN PATENT RIGHTS
WHICH MAY BE INVOLVED.

UNCLASSIFIED